Available online at www.sciencedirect.com
SCIENCE DIRECT®
ELSEVIER
Earth and Planetary Science Letters 217 (2004) 285–295
EPSL
www.elsevier.com/locate/epsl

Geomagnetic paleointensity and direct age determination of the ISEA (M0r?) chron

Rixiang Zhu [a,*], Kenneth A. Hoffman [b], Sébastien Nomade [c], Paul R. Renne [c,d], Ruiping Shi [a], Yongxin Pan [a], Guanghai Shi [a]

[a] *Laboratory of Paleomagnetism, Institute of Geology and Geophysics, Chinese Academy of Sciences, P.O. Box 9825, Beijing 100029, PR China*
[b] *Physics Department, California Polytechnic State University, San Luis Obispo, CA 93410, USA*
[c] *Berkeley Geochronology Center, 2455 Ridge Rd., Berkeley, CA 94709, USA*
[d] *Department of Earth and Planetary Science, University of California, Berkeley, CA 94720, USA*

Received 12 May 2003; received in revised form 11 October 2003; accepted 14 October 2003

Abstract

A combined paleomagnetic and geochronologic study has been conducted on an andesite lava sequence at Jianguo (Liaoning province, northeastern China). Thermal demagnetization and thermomagnetic analysis revealed that natural remanent magnetization is carried by both magnetite and hematite. Stepwise thermal demagnetization up to 675°C isolated well-defined reverse characteristic remanent magnetization (ChRM) in three time-independent lava flows with a mean direction of $D/I = 179.2°/-59.7°$ with $\alpha_{95} = 3.0°$. It also showed that a high-temperature component (> 585°C) has the same ChRM direction as that of the low- to medium-temperature (ca. 170/300–585°C) components. A modified version of the Thellier–Thellier paleointensity method [Coe, J. Geophys. Res. 72 (1967) 3247–3262] with systematic partial thermoremanent magnetization checks was used for paleointensity determinations. Twelve out of 39 samples yielded reliable results in the temperature interval of 170–550°C. Virtual dipole moment values range from 3.9 to 4.7×10^{22} Am^2 with an average of $4.2 \pm 0.1 \times 10^{22}$ Am^2. ^{40}Ar/^{39}Ar age determination on one lava flow is 116.8 ± 3.0 Myr (2σ error, relative to Fish Canyon sanidine: 28.02 ± 0.28 Myr). The magnetic reversed polarity with well-defined age could correspond to the 'ISEA' within the older part of the Cretaceous normal superchron (CNS), but we cannot rule out the possibility that this reversal interval could also correspond to the M0r due to many ambiguities on previous published ages on ISEA and M0r intervals as well as the new monitor age correction we applied. It also suggests that a weak magnetic field nature already documented before the CNS extended at least into the very beginning of the CNS.

Keywords: paleointensities; Ar-40/Ar-39 dating; ISEA (or M0r); China; andesite

1. Introduction

Despite the fact that brief episodes of reversed polarity within the Cretaceous normal superchron (CNS) have been reported [2–7], it has been dis-

* Corresponding author. Tel.: +86-10-62007912; Fax: +86-10-62010846.
E-mail address: rxzhu@mail.igcas.ac.cn (R. Zhu).

0012-821X/03/$ – see front matter © 2003 Elsevier B.V. All rights reserved.
doi:10.1016/S0012-821X(03)00613-7

puted whether a real reversed polarity chron occurred during the 'quiet' CNS. ISEA is the first documented fully reversed chron within the CNS, but it is not well defined magnetically [8], and blurred by imprecise and indirect absolute age control. Although the ISEA reversed polarity interval does not destroy the basic integrity of the CNS, it may aid resolution of the statistical structure of the geomagnetic reversal chron [6,9]. Besides the reversal, paleointensity values associated with the CNS are very important for constraining ancient geodynamo, but still remain scarce and controversial [10–12]. Towards these aims, a combination of paleomagnetic and geochronological researches has played a pivotal role [13].

Lavas are regarded as one of the best rock types from which reliable absolute paleointensities as well as $^{40}Ar/^{39}Ar$ ages can be obtained. In the present study we used a modified Thellier–Thellier method [1] for paleointensity determination combined with $^{40}Ar/^{39}Ar$ age determination on a Cretaceous andesitic lava sequence at Jianguo of the Fuxin-Yixian basin in the northeastern China. The lava flow recording a reversed polarity interval may correlate with the ISEA (or M0r?) chron, and correspond to weak magnetic field strength.

2. Geological setting and sampling

The Fuxin-Yixian basin is located in west Liaoning. This Mesozoic basin has attracted the attention of geologists and paleontologists because of the well-preserved and unique Early Cretaceous fossil assemblages, known as Jehol fauna, in its sedimentary strata [14,15]. Geologically, the uppermost rock unit of late Mesozoic time in this basin is named the Dalinghe (DLH) Formation, which mainly consists of gray-purplish andesites, pyroxene–andesite lavas and blackish basalts. Based on the fossil assemblages in the underlying Sunjiawan Formation, e.g. *Acanthopteris onychioides* (Vassil.) Zhang, *Ginkgoites* sp., *Elatocladus* cf. *manchurica* (Yok.), *Coniopteris* sp. [16], the DLH Formation has been accepted as a volcanic eruption production of mid-Cretaceous age [17]. Yet so far no radiometric dating has been reported on those volcanic rocks. Furthermore, it has been documented that the latitude of the studied section has no obvious changes since the DLH Formation formed [12,16].

The Jianguo (JG) section (42°16.7′N, 121°54.3′E) is located in the northern part of the Fuxin-Yixian basin. The DLH formation at this section is composed of ~40 m gray-greenish or gray-purplish andesite and pyroxene–andesite lavas. No sedimentary horizons have been distinguished between these flows. Using vesicular zones and scoria, five lava flows (JG13–JG17) were identified, with a thickness of 6 m, 10 m, 7 m, 6 m and >11 m, respectively. At least eight cores, orientated in situ using magnetic compass and sun compass, were taken from each lava using a gasoline-powered diamond drill. Two/three paleomagnetic samples were trimmed from each core. The underlying Sunjiawan Formation strata are very poorly cemented and unsuitable for paleomagnetic sampling, but helpful to evaluate the strike/dip of the lava flows. Other Early Cretaceous rock units were covered by Quaternary deposits in the vicinity of the sampling site. Although a fresh massive sample was collected from each lava flow for radiometric dating, only JG13 was suitable for $^{40}Ar/^{39}Ar$ dating. The other samples presented very fine-grained texture as well as pervasive alteration. Both of these problems could lead to various artifacts (recoil, argon loss) and as a consequence to biased ages.

3. $^{40}Ar/^{39}Ar$ analytical methods and result

One fresh fine-grained andesite (sample number JG13) was chosen for $^{40}Ar/^{39}Ar$ geochronology. The rock was crushed, sieved and the selected fraction (mesh 40–60 (230–380 μm)) was washed several times in distilled water in an ultrasonic cleaner. Olivine phenocrysts were removed after two passes through a magnetic separator operating at 0.5 A. From this cleaned fraction we separated only fresh groundmass mainly composed of fine laths of plagioclase (20–60 μm), pyroxenes and magnetite. A total of 15 mg were loaded in an aluminum disk as described by Renne et al. [18] and irradiated for 5 h in the CLICIT facility

of the TRIGA reactor at Oregon State University. After irradiation, 30 grains were degassed with a defocused CO_2 laser then analyzed with a MAP 215C mass spectrometer at the Berkeley Geochronology Center using methods also described by Renne et al. [19].

Procedural blanks were measured every three steps and typical values (in mol) were $(1.0\pm0.1)\times10^{-16}$ for ^{40}Ar, $(5.5\pm0.9)\times10^{-18}$ for ^{39}Ar, $(2.4\pm0.8)\times10^{-19}$ for ^{38}Ar, $(3.5\pm0.6)\times10^{-18}$ for ^{37}Ar, $(7.4\pm1.0)\times10^{-18}$ for ^{36}Ar and values of the unknown of 6.4×10^{-14} for ^{40}Ar, 1.2×10^{-15} for ^{39}Ar, 2.4×10^{-18} for ^{38}Ar, 4.2×10^{-16} for ^{37}Ar, 1.3×10^{-17} for ^{36}Ar. Neutron fluence (J) was monitored by Fish Canyon sanidine (FCs: 28.02 Myr, Renne et al. [18]) grains in four positions in the aluminum disk. The J value for the disk was determined from individual analyses of six separate FCs grains in each position fused with the CO_2 laser (total of 24 grains). The corresponding J values calculated with the total decay constant of Steiger and Jäger [20] is 0.0013309 ± 0.000006. The error in J is calculated excluding systematic contributions to age uncertainties from the standard and the decay constant. Mass discrimination, monitored by automated analysis of air pipettes interspersed with the unknown (each nine steps), was 1.00648 ± 0.0039 (2σ error) per mass atomic unit. Nucleogenic production ratios from K and Ca were $(^{40}Ar/^{39}Ar)_K = 0.00073\pm9.10^{-5}$, $(^{39}Ar/^{37}Ar)_{Ca} = 0.00076\pm0.000085$, $(^{36}Ar/^{37}Ar)_{Ca} = 0.00027\pm2.10^{-6}$. The plateau age is defined as comprising three contiguous steps corresponding to at least 50% of the total ^{39}Ar released, where individual fraction ages agree within 2σ of the weighted mean age of the plateau segment.

Fig. 1 shows the $^{40}Ar/^{39}Ar$ apparent age, K/Ca ratio spectra, isochron plot and isochron age. All errors are reported at the 2σ level. The spectrum is discordant, characterized by rising ages in the first 20% of ^{39}Ar released, followed by a flat zone (75% of the total ^{39}Ar) which yields a plateau age of 118.9 ± 1.1 Myr. Such behavior in fine-grained materials is commonly due to the degassing of younger alteration products and the flat zone likely corresponds to the degassing of plagioclase. Commonly, groundmass spectra display discordant younger ages corresponding to the degassing of ^{39}Ar implanted into refractory minerals such as pyroxene, where it is unsupported by $^{40}Ar^*$. In our case, such behavior is not evident. Nevertheless, degassing of a Ca-rich, K-poor phase (pyroxene) at high temperatures is indicated by the decreasing K/Ca ratio. At low temperatures, low apparent ages are associated with small variation of the K/Ca ratio. This indicates a contribution from K-rich secondary phases (e.g. clays). The isotope correlation diagram (isochron, right panel of Fig. 1) indicates a trapped initial $^{40}Ar/^{36}Ar$ ratio of 415 ± 140 (2σ error), defined by steps F–X). Including additional steps, which we interpret to reflect alteration effects, produces excess scatter (MSWD > 2) and thus no longer defines a valid isochron. The plateau and isochron ages are not statistically distinct. Nevertheless we regard the isochron age as being more objective, as no assumptions are made about the initial $^{40}Ar/^{36}Ar$

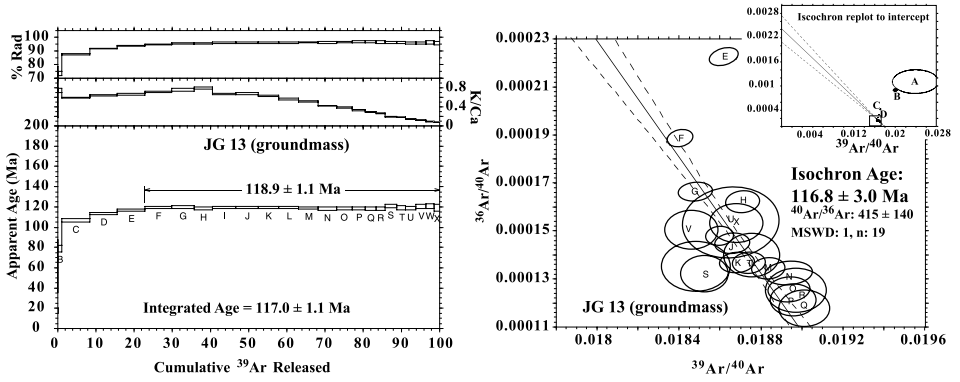

Fig. 1. Apparent age spectrum with K/Ca ratio and isochron for sample JG13. All errors are reported at 2σ level.

ratio or its uncertainty. Therefore, we interpret the isochron age (116.8 ± 3.0 Myr; 2σ error, MSWD = 1) as yielding the most objective age estimate for this sample. The age uncertainty does not include systematic errors related to standards or the ^{40}K decay constants, which should be considered if this result is compared to age estimates obtained from other radioisotopic systems (e.g. [21]).

4. Paleomagnetic analysis

4.1. Paleodirectional results

Stepwise thermal cleaning involving a minimum of 12 steps up to 585°C/675°C was performed on a total of 32 samples (one from each core) for paleodirectional determination using a Magnetic Measurements thermal demagnetizer with a residual magnetic field less than 10 nT. Remanence measurements were conducted on a JR-5A spinner magnetometer situated in a field free space (< 300 nT). Typical demagnetization diagrams are shown in Fig. 2. The majority of the samples (28 out of 32) are characterized by a stable component isolated after demagnetization at a low temperature (170–300°C). The characteristic direction was determined using least-squares methods [22] (Fig. 2), and interpreted as the characteristic remanent magnetization (ChRM). The mean directions and the number of samples per flow are listed in Table 1 with the 95% circle of confidence, the precision parameter and the corresponding latitude and longitude of the virtual geomagnetic poles (VGP). The results showed that all five lava flows recorded a reversed polarity.

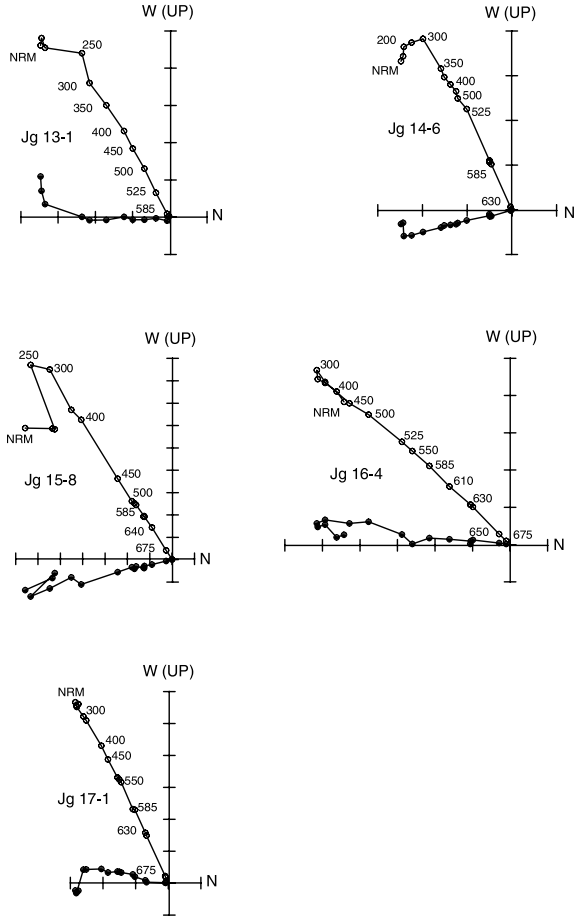

Fig. 2. Orthogonal projections of representative progressive thermal demagnetization. The solid (open) symbols refer to the horizontal (vertical) plane.

Table 1
Paleodirectional results from Jianguo section

Lava#	*n*/*N*	*D* (°)	*I* (°)	*k*	α_{95} (°)	PLA (°)	PLO (°)	*D* (°)	*I* (°)	*k*	α_{95} (°)	PLA (°)	PLO (°)
JG13	6/6	175.1	−58.5	190.9	4.9	−85.2	173.8	175.1	−58.5	190.9	4.9	−85.2	173.8
JG14§	5/6	190.6	−60	165.1	6	−82	38.4						
JG15§	6/7	191.4	−57.1	100.2	6.7	−80.1	55.9	189.9	−59.1	130.1	3.2	−82.2	46.6
JG16§	5/6	187.2	−60.5	118.3	7.1	−84.6	38.3						
JG17	6/7	172.5	−60.9	110.3	6.4	−84.4	210.7	172.5	−60.9	110.3	6.4	−84.4	210.7
Mean								179.2	−59.7	272.2	3.0	−88.2	141.1

Note: *n*/*N*, number of samples (28) used in the paleodirection calculation/total number of samples (32) demagnetized; *D*/*I*, declination/inclination; α_{95}, radius of circle of the 95% confidence about the direction; PLA/PLO, VGP latitude/longitude; Symbol § stands for paleomagnetically indistinguishable lava flows.

Although five lava flows were identified in the field based on vesicular and scoria, an *F*-test [23] to compare the mean directions of adjacent individual flows indicated that lavas JG14, JG15 and JG16 were indistinguishable. These paleomagnetically related lava flows may imply either subsequent eruption in relatively short time intervals and/or flow number overestimation in field. Thus these three lavas were combined as JG14–16 in further analysis. The calculated mean direction of JG14–16 is $D = 189.9°/I = -59.1°$ ($\alpha_{95} = 3.2°$). Mean directions determined from three time-independent lava flows, JG13, JG14–16 and JG17, are $D = 179.2°/I = -59.7°$ ($\alpha_{95} = 3.0°$) and its corresponding VGP latitude and longitude are −88.2° and 141.1°, respectively.

4.2. Magnetic minerals and sample selection

Thermomagnetic analysis and electron microscopy observation were performed on whole rock samples to characterize the magnetic carriers and guide sample selection for paleointensity experiments. Thermomagnetic measurements were conducted in argon atmosphere on a variable field translation balance with heating and cooling rates of 12°/min, while applying a field of 200 mT. The Curie temperatures were determined by extrapolating graphically the successive changes in the slopes of the heating curves [24]. Fig. 3 shows that magnetic remanence carriers of those rocks are a mixture of 'soft' magnetite and 'hard' hematite. Samples with nearly reversible behaviors of heating and cooling curves (thermally stable) were selected for paleointensity experiments and 'irreversible' behavior samples were discarded.

Before carrying out paleointensity experiments, it must be determined whether the hematite is 'primary' or weathering-derived as secondary product may carry a chemical remanent magnetization and as a consequence invalidate Thellier paleointensity experiments [25]. Electron microscope observations on polished thin sections indicated that the minerals including Fe-minerals and plagioclase, with well-crystallized euhedral crystals, did not undergo metasomatic reactions or inversions after these rocks formed (Fig. 4), suggesting that hematite was likely formed by primary high-temperature oxidation of titanomagnetite during cooling from the melt.

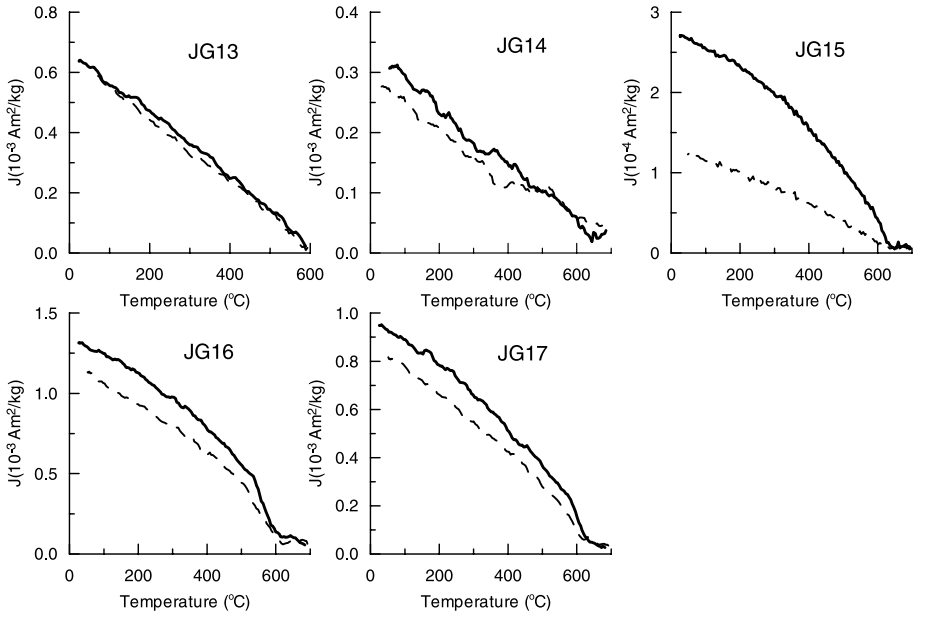

Fig. 3. Representative results of thermomagnetic curves (*J*–*T*) of samples from each field lava flow at Jianguo section. Solid and dashed lines stand for the heating and cooling curves, respectively.

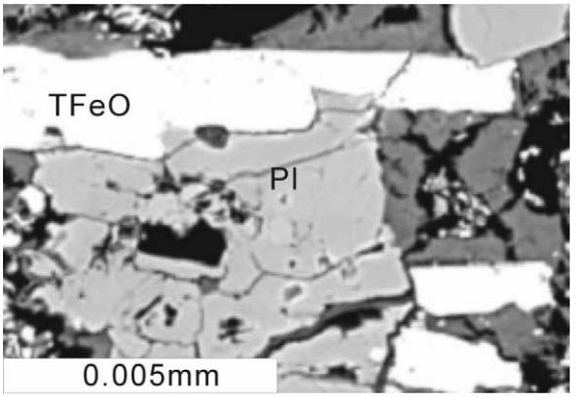

a)

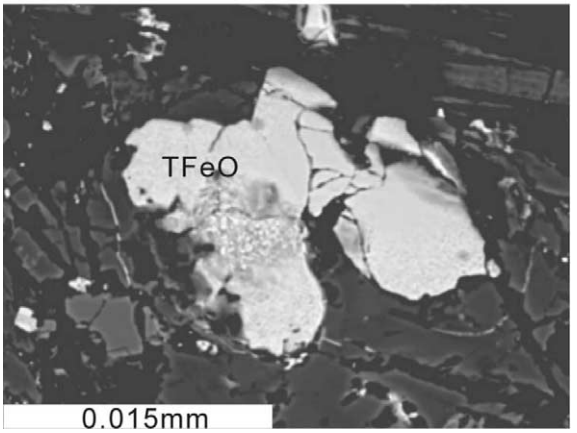

b)

Fig. 4. Backscatter electron images of 'primary' textures and Fe-minerals. TFeO: Fe-minerals (Fe_3O_4+$Fe_2O_3 \pm Fe_2TiO_4$), Pl: plagioclase; the dark phase: glass matrix. (a) JG17; (b) JG13.

4.3. Paleointensity determinations

The paleointensity experiments were carried out in the Laboratory of Paleomagnetism at the Institute of Geology and Geophysics (Beijing). A modified version [1] of the original Thellier–Thellier [26] double heating paleointensity method was used in this study, with a 50 μT laboratory field applied during both the heating and cooling cycles. In order to heat the samples rapidly, yet not overshoot the desired peak temperature, a non-linear heating ramp was employed. Specifically, a rate of 3.2°C/min was applied until the temperature in the furnace reached the final

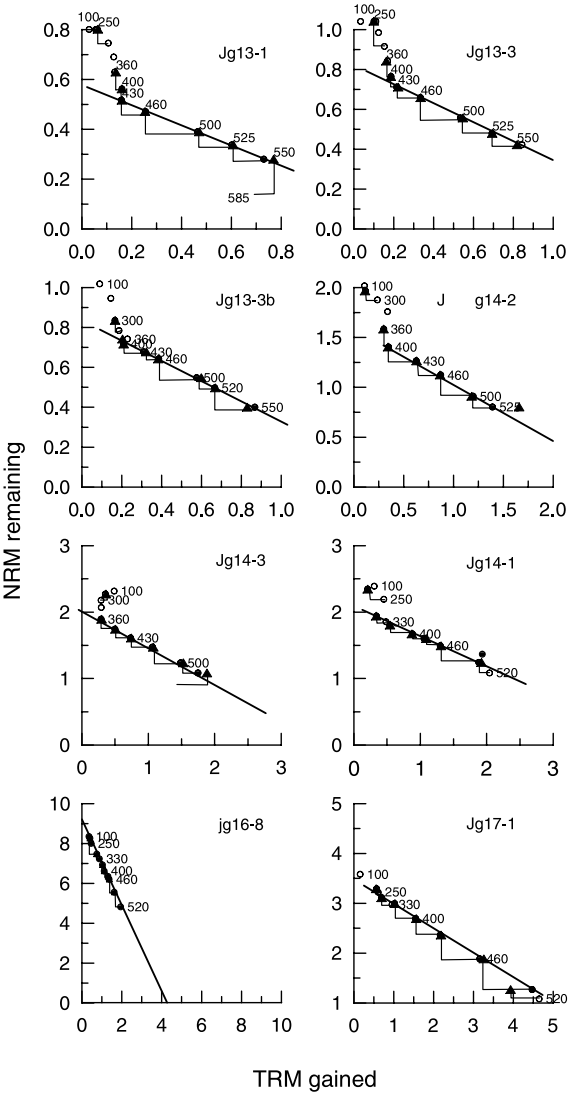

Fig. 5. Examples of reliable NRM–TRM diagrams used for paleointensity determinations. Filled (open) circles denote data points accepted (rejected) from the best-fit line used to define the paleointensity value; triangles are pTRM checks. The numbers refer to temperatures in °C.

60°C mark at which point a slower heating rate of 1°C/min was used until the target temperature was obtained. The samples were then held at that temperature for 30 min in order for thermodynamic equilibrium to be reached. The samples were then allowed to cool naturally overnight. In order to minimize possible chemical alteration during heating, prior to each run air was first

evacuated from the furnace with a primary vacuum pump. Then argon was alternately flushed in and pumped out of the chamber several times. A gentle stream of argon was then maintained during the entire experiment [27].

A total of 39 samples from these lava flows were chosen for whole rock Thellier–Thellier paleointensity experiments. To determine the temperature interval over which reliable paleointensity estimates could be obtained from the studied samples, we used a set of selection criteria, which are similar to those published in the literature [10,28]. Representative results are shown in Fig. 5, and the natural remanent magnetization (NRM) remaining at each temperature is plotted against the corresponding partial thermoremanent magnetization (pTRM) acquired in the laboratory field at the same temperature. Data were considered reliable up to the temperature at which magnetochemical changes started to occur, indicated by non-linearity in the NRM–TRM curve and negative pTRM checks. pTRM checks were taken as negative when the new pTRM value at a given temperature varied from the previous one by 5% of the initial NRM. In the Arai diagrams, slopes defined by fewer than four points and corresponding to the removal of less than 30% of the total NRM (i.e. $f < 0.3$) were not used for paleointensity estimates. The determinations were considered to be reliable only if more than three positive pTRM checks were reached.

Twelve samples yielded apparently reliable paleointensity results, with a sample success rate of 30%. We noted that the samples yielding linear Arai diagrams were also characterized by high directional stability, with no tendency for the magnetization to align along the laboratory field. This indicates that the chemical remanent magnetization produced during heating is not significant [29,30]. The mean paleointensity values per flow obtained range from 22.1 to 27.1 μT (see Table 2).

5. Discussion and conclusions

5.1. The primary origin of magnetization

Before we try to interpret the full-vector paleomagnetic data from the Jianguo section, it is critical to consider whether the magnetization is of primary origin. As discussed before, thermomagnetic analysis and electron microscope observa-

Table 2
Paleointensity determinations and associated statistical parameters

Sample	n	T_{int}	f	Gap	q	$F \pm \sigma$ (μT)	$Fa \pm \sigma_F$ (μT)	$VDM \pm \sigma_v$ (10^{22} Am^2)
JG13-1	5	430–550	0.409	0.737	17.114	20.36 ± 0.44		
JG13-3	5	430–550	0.356	0.732	9.966	23.51 ± 0.76		
JG13-3b	6	400–550	0.384	0.764	15.669	24.52 ± 0.57	22.1 ± 1.3	3.9 ± 0.29
JG14-1§	7	300–500	0.336	0.782	10.016	21.99 ± 0.71		
JG14-2§	5	400–525	0.371	0.734	10.161	29.32 ± 0.97		
JG14-3§	6	360–525	0.399	0.789	10.77	26.89 ± 0.97		
JG16-1§	8	250–500	0.562	0.78	24.855	25.01 ± 0.55		
JG16-3§	10	170–500	0.595	0.821	41.221	27.39 ± 0.40		
JG16-5§	10	170–500	0.602	0.819	24.483	30.45 ± 0.76		
Combined from §							27.1 ± 1.3	4.7 ± 0.2
JG17-1	8	250–500	0.335	0.763	4.275	25.50 ± 1.89		
JG17-2	9	200–500	0.646	0.817	11.268	24.55 ± 1.42		
JG17-4	9	200–500	0.356	0.826	7.164	22.37 ± 1.14	24 ± 0.9	4.1 ± 0.2
Site mean paleointensity 24.4 ± 0.7							Site mean VDM 4.2 ± 0.1	

n, T_{int}: the number of points and the temperatures defining the linear segment; f: the percentage of the NRM used for the determination; g: an index of how well the NRM–TRM points are distributed along a straight line segment; q: quality factor defined by function $|b| \cdot f \cdot g/\sigma(b)$ where b is the slope and $\sigma(b)$ is its standard deviation [28]; $F \pm \sigma$: paleointensity estimate for individual samples and standard error; $Fa \pm \sigma_F$, mean paleointensity and its standard error for each lava; $VDM \pm \sigma_v$: virtual dipole moment and standard error. Symbol § stands for the samples taken from paleomagnetically indistinguishable lava flows.

tion show that the remanence is mainly carried in most cases by Ti-poor titanomagnetite, which most probably indicates thermoremanent origin of primary magnetization [31]. Some samples contain a high degree of deuteric oxidation-produced hematite. We also performed a crude reversal test [32] on results of this study and another lava sequence of similar age (56 km southwest of the JG section) from the same basin. The mean ChRM direction obtained in this study ($D = 179.2°/I = -59.7°$ with $\alpha_{95} = 3.0°$) is nearly anti-parallel to the mean direction ($D = 5.4°/I = 58.7°$ with $\alpha_{95} = 2.4°$) determined from 15 normally magnetized lava flows with K–Ar ages of 133–124 Myr [12]. Thus, we are confident that the ChRM directions can be regarded as primary in origin, even though application of a fold test on these flows was not possible. Moreover, we compare our data with previous studies on basalts and tuffs from Inner Mongolia along the western part of the Tanlu fault [33], in which it was demonstrated that the remanent magnetization of the rock units was of primary origin, since the ChRM directions passed both fold and reversal tests. [33] found the mean Early Cretaceous paleodirection associated with the studied region to be $D/I = 6.8°/58.5°$, corresponding to a paleopole near the present rotation axis at 82.9°N latitude, 249.5°E longitude. Our results are virtually identical to Zhao et al.'s [33] findings, which partly suggests that data from the studied section are dominated by a dipole component. It needs to be kept in mind, however, that the averaged paleofield values obtained are not necessarily free of effects caused by an insufficiently averaged paleosecular variation because only three time-independent lava flows were measured. It is also noted that the mean VGP from these lava flows, lying ~15° away from the apparent polar wander paths of Eurasia in the same time interval [34], is not necessarily free of regional deformation. But no significant latitudinal placement was revealed within 95% confidence. Put another way, it is reasonable to calculate the VDM.

5.2. ISEA or M0r?

The isochron age of lava JG13 is apparently younger than the age of the M0r event (121 ± 1.4 Myr; Barremian/Aptian boundary) but is close to the age of the ISEA interval (ca. 115 Myr; Upper Aptian) proposed by Gradstein et al. [35]. Nevertheless, as recently pointed out [36], the absolute ages of the M0r and ISEA chrons are still unclear and an overview of available relevant $^{40}Ar/^{39}Ar$ ages reveals discrepancies which must be taken into account in order to discuss the age we obtained in an appropriate context, and in order to meaningfully evaluate the absolute ages of these two chrons.

The M0r age constraint is based on data published by Pringle and Duncan [37]. More specifically, lavas close to the base of M0r yielded an age of 119.6 ± 1.4 Myr (2σ error). This age is the weighted mean of three $^{40}Ar/^{39}Ar$ isochron ages (four to five steps) ranging from 120.7 ± 2.8 to 117.1 ± 4 Myr (2σ error) which could come from distinct flows. These ages were reported relative to an age of 27.92 ± 0.04 Myr for the Taylor Creek Rhyolite sanidine (TCRs) which is about 1.5% younger than the age proposed by [18]. In order to compare our age with this work, we have recalculated ages individually according to the standard TCRs at 28.34 ± 0.28 Myr, consistent with the FCs at 28.02 ± 0.28 Myr [18]. After correction, the weighted mean age of [37] becomes 121.4 ± 1.6 Myr. This age as well as the age proposed by [35] should be considered as approximations of the maximum age of the base of the M0r chron. Even if this weighted mean age is statistically older than the age we obtained, it is not distinct from the younger age obtained by [35] recalculated herein to 118.9 ± 4.2 Myr. Recently, Gilder et al. [36] proposed an age of 113.3 ± 3.2 Myr (2σ error) [38] for the M0r (or ISEA). Nevertheless, the age spectra (see fig. 4 in [38]) display typical recoil features and should be considered with caution. Moreover, this age is relative to the TCRs at 27.92 ± 0.04 Myr and should be recalculated at 115.0 ± 3.4 Myr (using TCRs at 28.34 ± 0.28 Myr). This age is statistically indistinguishable from the age we obtained for JG13 (116.8 ± 3.0 Myr; MSWD = 1).

The previously inferred age of the ISEA (ca. 115 Myr) [35] is based on an extrapolation from the M0r age estimation to the Albian/Aptian limit

(112.2 ± 1.1 Myr) [36]. The only geochronological control is the age obtained on basalt at the base of site 879 (Takuyo–Daisan Guyots) [37] and located above the M0r chron but below the ISEA chron which gives an age of 119.9 ± 2.6 Myr (2σ level; recalculated with the TCRs at 28.34 ± 0.28 Myr). Our study provides unambiguous evidence of a reverse polarity interval with a well-defined age of 116.8 ± 3.0 Myr. Unfortunately, due to many ambiguities on previous published ages on ISEA and M0r intervals as well as the new monitor age correction we applied, we cannot rule out the possibility that this reversal interval could also correspond to the M0r. However, if it is ISEA, this occurrence would be the first such recording in continental lavas with direct $^{40}Ar/^{39}Ar$ age control.

5.3. Paleointensity and the CNS

Even after pre-selection, 27 samples (i.e. 70%) did not give reliable intensity results. The causes of the failure are probably intrinsic to andesite rocks using the Thellier–Thellier method [39]. Magnetic mineral alteration during laboratory heating is undoubtedly the main source of error in paleointensity determination. The Thellier laws break down if multidomain magnetic grains are produced during heating [40]. We also note that the NRM drops off below 400°C with little TRM acquisition (Fig. 5), which could be due to destruction of maghemite and decay of viscous remanence, but no maghemitization was observed from thermomagnetic analysis and electron microscope observation.

Although the CNS provides an opportunity to view the geomagnetic field in an extreme state regarding reversal frequency [41], the long-term variation in the strength of the geodynamo is still poorly understood given the paucity of available reliable paleointensity data in space and time. The calculated mean VDM value of $(4.2 \pm 0.1) \times 10^{22} Am^2$ of this study is remarkably consistent with previously published data from the Zhuanchengzi and Sihetun sections dated at 120.93 ± 0.88 Myr [42] and 133–124 Myr [12]. The findings suggest extension of the relatively low nature of the pre-CNS magnetic field strength into the very beginning of the CNS (Fig. 6). A relationship between reversal rate and paleointensity remains a contentious topic in the study of the geodynamo, though Zhu et al. [12] proposed that variation of the averaged paleointensity data, spanning some 40 Myr or more of field behavior just prior to the onset of the CNS, exhibits an increasing trend as the CNS is approached. In fact, two main interpretations have been advanced for the evolution of the geomagnetic reversal rate since 160 Myr [43–45]. McFadden and Merrill [44] inferred a long-term decrease of the reversal rate over the ~40 Myr period preceding the CNS, while other authors have concluded no such change preceded the sudden occurrence of the CNS [43,45]. It is obvious that these two views have quite different implications for the reversal process. Neither interpretation can be rejected on statistical grounds [46]. As shown in Fig. 6, no significant 'precursor' can be resolved as a discontinuity before the onset of the CNS based on the geomagnetic strength behavior from 162 Myr to the very beginning of this superchron. It should be noted, however, that when a time-averaged VDM of $(12.5 \pm 1.4) \times 10^{22}$ Am^2 covering the time interval from 116 Myr to 113 Myr [11] is considered, the VDM behavior seems to gradually increase from its value of

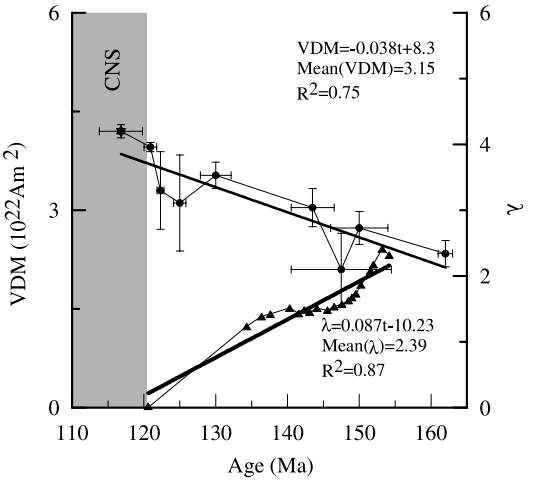

Fig. 6. Relationship between the long-term variations of the Earth's magnetic field strength (VDM) and rates of reversal frequency (λ) spanning the time interval from 165 Myr to 116 Myr. Modified from [12]. The star stands for the VDM determined in this study.

about $(2.3 \pm 0.2) \times 10^{22}$ Am^2 at about 162 Myr to $(4.2 \pm 0.1) \times 10^{22}$ Am^2 at about 116.8 Myr (ISEA?), and then displays a rapid increase between 116 Myr and 113 Myr. This suggests that the state of the geodynamo experienced a sudden change at about the time of the ISEA. Thus clarifying the evolution of geomagnetic strength during the CNS becomes very important. Thus far, reported VDMs inside the CNS are quite inconsistent (see e.g. [10,11,41,47–49]), suggesting that more paleointensity estimates with precise ages are needed before we can conclude high or low strengths during the CNS.

Acknowledgements

The authors would like to thank Vincent Courtillot, Peter Riisager and two anonymous reviewers for their constructive suggestions. This work was supported by the NKBRSF project of China (G1999075509), the National Science Foundation of China (40221402) and CAS (KZCX1-07). *[VC]*

References

[1] R.S. Coe, Palaeo-intensities of the earth's magnetic field determined from Tertiary and Quaternary rocks, J. Geophys. Res. 72 (1967) 3247–3262.
[2] B. Keating, C.E. Helsley, Paleomagnetic results from DSDP Hole 391 and the magnetostratigraphy of Cretaceous sediments from the Atlantic Ocean floor, Init. Rep. DSDP 44 (1978) 523–528.
[3] J. VandenBerg, C.T. Klootwijk, A.A.H. Wonders, The Late Mesozoic and Cenozoic movements of the Umbrian Peninsula: Further paleomagnetic data from the Umbrian sequence, Geol. Soc. Am. Bull. 89 (1978) 133–155.
[4] J. VandenBerg, A.A.H. Wonders, Paleomagnetism of Late Mesozoic pelagic limestones from the Southern Alps, J. Geophys. Res. 85 (1980) 3623–3627.
[5] J. Urrutia-Fucugauchi, Paleomagnetic study on the Cretaceous Morelos Formation, Guerrero State, Southern Mexico, Tectonophysics 147 (1988) 121–125.
[6] J.A. Tarduno, Brief reversed polarity internal during the Cretaceous Normal Polarity Superchron, Geology 18 (1990) 683–686.
[7] J.A. Tarduno, W. Lowrie, W.V. Sliter, T.J. Bralower, F. Heller, Reversed polarity characteristic magnetizations in the Albian Contessa section, Umbrian Apennines, Italy: Implications for the existence of a Mid-Cretaceous mixed polarity interval, J. Geophys. Res. 97 (1992) 241–271.
[8] M. Cronin, L. Tauxe, C. Constable, P. Selkin, T. Pick, Noise in the quiet zone, Earth Planet. Sci. Lett. 190 (2001) 13–30.
[9] J.A. Tarduno, W.V. Sliter, T.J. Bralower, M. McWiams, I.P. Silva, J.G. Ogg, M-sequence reversals recorded in DSDP sediment cores from the western Mid-Pacific Mountains and Magellan Rise, Geol. Soc. Am. Bull. 101 (1989) 1306–1316.
[10] T. Pick, L. Tauxe, Geomagnetic palaeointensities during the Cretaceous normal superchron measured using submarine basaltic glass, Nature 366 (1993) 238–242.
[11] J.A. Tarduno, R.D. Cottrell, A.V. Smirnov, High geomagnetic intensity during the Mid-Cretaceous from Thellier analyses of single plagioclase crystals, Science 291 (2001) 1779–1783.
[12] R.X. Zhu, K.A. Hoffman, Y.X. Pan, R.P. Shi, D.M. Li, Evidence for weak geomagnetic field intensity prior to the Cretaceous normal superchron, Phys. Earth Planet. Inter. 136 (2003) 187–199.
[13] B.S. Singer, K.A. Hoffman, A. Chauvin, R.S. Coe, M.S. Pringle, Dating transitionally magnetized lavas of the late Matuyama Chron: Toward a new ^{40}Ar/^{39}Ar timescale of reversals and events, J. Geophys. Res. 104 (1999) 679–693.
[14] Y.X. Pan, R.X. Zhu, J. Shaw, Y.X. Zhou, Magnetic polarity ages of the fossil-bearing strata at the Sihetun Section, West Liaoning: A preliminary result, Chin. Sci. Bull. 46 (2001) 680–684.
[15] Z.H. Zhou, P.M. Barrett, J. Hilton, An exceptionally preserved Lower Cretaceous ecosystem, Nature 421 (2003) 807–814.
[16] Bureau of Geology and Mineral Resources of the Liaoning Province, Regional Geology of Liaoning Province, Geological Publishing House, Beijing, 1989.
[17] Bureau of Geology and Mineral Resources of Liaoning, Regional Geology Map of Yixian, First Group of Regional Geology Survey of Liaoning, 1970, pp. 1–52.
[18] P.R. Renne, C.C. Swisher, A.L. Deino, D.B. Karner, T.L. Owens, D.J. DePaolo, Intercalibration of standards, absolute ages and uncertainties in ^{40}Ar/^{39}Ar dating, Chem. Geol. 145 (1998) 117–152.
[19] P.R. Renne, W.D. Sharp, A.L. Deino, G. Orsi, L. Civetta, ^{40}Ar/^{39}Ar Dating into the historical realm: Calibration against Pliny the Younger, Science 277 (1997) 1279–1280.
[20] R.H. Steiger, E. Jäger, Subcommission on geochronology: convention on use of decay constants in geo- and cosmochronology, Earth Planet. Sci. Lett. 36 (1977) 359–362.
[21] F. Begemann, K.R. Ludwig, G.W. Lugmair, K. Min, L.E. Nyquist, P.J. Patchett, P.R. Renne, C.-Y. Shih, I.M. Villa, R.J. Walker, Call for an improved set of decay constants for geochronological use, Geochim. Cosmochim. Acta 65 (2001) 111–121.

[22] J.L. Kirschvink, The least-square line and plane and analysis of paleomagnetic data, Geophys. J. R. Astron. Soc. 62 (1980) 699–718.
[23] P. McFadden, F.J. Lowes, The discrimination of mean directions drawn from Fisher distributions, Geophys. J. R. Astron. Soc. 67 (1981) 19–33.
[24] B.M. Moskowitz, Methods for estimating Curie temperatures of titanomagnetites, Earth Planet. Sci. Lett. 53 (1981) 84–88.
[25] P. Riisager, J. Riisager, N. Abrahamsen, R. Waagstein, Thellier palaeointensity experiments on Faroes flood basalts: technical aspects and geomagnetic implications, Phys. Earth Planet. Inter. 131 (2002) 91–100.
[26] E. Thellier, O. Thellier, Sur l'intensité du champ magnétique terrestre dans le passé historique et géologique, Ann. Géophys. 15 (1959) 285–376.
[27] C. Laj, N. Szeremeta, C. Kissel, H. Guillou, Geomagnetic paleointensities at Hawaii between 3.9 and 2.1 Ma: preliminary results, Earth Planet. Sci. Lett. 179 (2000) 191–204.
[28] R.S. Coe, C.S. Grommé, E.A. Mankinen, Geomagnetic paleointensities from radiocarbon-dated lava flows on Hawaii and the question of the Pacific nondipole low, J. Geophys. Res. 83 (1978) 1740–1756.
[29] C. Laj, C. Kissel, Geomagnetic field intensity at Hawaii for the last 420 kyr from the Hawaii Scientific Drilling Project core, Big Island, Hawaii, J. Geophys. Res. 104 (1999) 15317–15338.
[30] J. Carlut, X. Quidelleur, Absolute palaeointensities recorded during the Brunhes chron at La Guadeloupe Island, Phys. Earth Planet. Inter. 120 (2000) 255–269.
[31] A.L. Goguitchaichvili, M. Alva-Valdivia, J. Rosas-Elguera, J. Urrutia-Fucugauchi, J.A. Gonzalez, J. Morales, J. Sole, An integrated paleomagnetic study of Rio Grande de Santiago volcanic succession (trans-Mexican volcanic belt): revisited, Phys. Earth Planet. Inter. 130 (2002) 175–194.
[32] P.L. McFadden, M.W. McElhinny, Classification of the reversal test in palaeomagnetism, Geophys. J. Int. 103 (1990) 725–729.
[33] X. Zhao, R.S. Coe, Y.X. Zhou, H.R. Wu, J. Wang, New paleomagnetic results from northern China collision and suturing with Siberia and Kazakhstan, Tectonophysics 181 (1990) 43–81.
[34] J. Besse, V. Courtillot, Apparent and true polar wander and the geometry of the geomagnetic field over the last 200 Myr, J. Geophys. Res. 107 (2002) 10.1029/2000JB000050.
[35] F.M. Gradstein, F.P. Agterberg, J.G. Ogg, J. Hardenbol, P. Van Veen, J. Thierry, Z. Huang, A Triassic, Jurassic and Cretaceous Time Scale, in: W.A. Berggren et al. (Eds.), Geochronology, Time Scales and Global Stratigraphic Correlation, SEPM Spec. Publ. 54 (1995) 95–126.
[36] S. Gilder, Y. Chen, J.P. Cogné, X. Tan, V. Courtillot, D. Sun, Y. Li, Paleomagnetism of Upper Jurassic to Lower Cretaceous volcanic and sedimentary rocks from the western Tarim Basin and implications for inclination shallowing and absolute dating of M-0 (ISEA?) Chron, Earth Planet. Sci. Lett. 206 (2003) 587–600.
[37] M.S. Pringle, R.A. Duncan, Radiometric ages of basement lavas recovered at Loen, Wodejebato, MIT, and Takuyo-Daisan Guyots, Northwestern Pacific Ocean, Proc. ODP Sci. Results 144 (1995) 547–557.
[38] E.R. Sobel, N. Arnaud, Cretaceous-Paleogene basaltic rocks of the Tuyon basin, NW China and Kyrgyz Tian Shan: The trace of a small plume, Lithos 50 (2000) 191–215.
[39] A.A. Kosterov, M. Prevot, Possible mechanisms causing failure of Thellier palaeointensity experiments in some basalts, Geophys. J. Int. 134 (1998) 554–572.
[40] E. McCleland, Theory of CRM acquired by grain growth, and its implications for TRM acquisition and paleointensity determinations in igneous rocks, Geophys. J. Int. 126 (1996) 271–280.
[41] J.A. Tarduno, R.D. Cottrell, A.V. Smirnov, The Cretaceous superchron geodynamo: Observations near the tangent cylinder, Proc. Natl. Acad. Sci. USA 99 (2002) 14020–14025.
[42] R.X. Zhu, Y.X. Pan, J. Shaw, D.M. Li, Q. Li, Geomagnetic palaeointensity just prior to the Cretaceous Normal Superchron, Phys. Earth Planet. Inter. 128 (2001) 207–222.
[43] Y. Gallet, G. Hulot, Stationary and nonstationary behaviour within the geomagnetic polarity time scale, Geophys. Res. Lett. 24 (1997) 1875–1878.
[44] P.L. McFadden, R.T. Merrill, Evolution of the geomagnetic reversal rate since 160 Ma: Is the process continuous?, J. Geophys. Res. 105 (2000) 28455–28460.
[45] G. Hulot, Y. Gallet, Do superchrons occur without any palaeomagnetic warning?, Earth Planet. Sci. Lett. 210 (2003) 191–201.
[46] C. Constable, On rates of occurrence of geomagnetic reversals, Phys. Earth Planet. Inter. 118 (2000) 181–193.
[47] M.T. Juarez, L. Tauxe, J.S. Gee, T. Pick, The intensity of the Earth's magnetic field over the last 160 million years, Nature 394 (1998) 878–881.
[48] V.P. Shcherbakov, G.M. Solodovnikov, N.K. Sycheva, Variations in the geomagnetic dipole during the past 400 million years (Volcanic rocks), Izv. Phys. Solid Earth 38 (2002) 113–119.
[49] H. Tanaka, M. Kono, Paleointensities from a Cretaceous basalt platform in Inner Mongolia, northeastern China, Phys. Earth Planet. Inter. 133 (2002) 147–157.